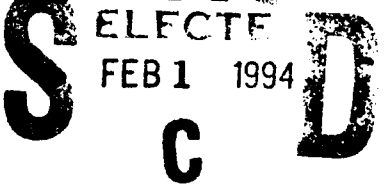

(2)

N00014-93-1-0080

First Annual Report on ONR Grant ~~N-00014-93-0080~~

A Study of Solid Propellants using a Microprobe Mass Spectrometer System

Thomas A. Litzinger
Penn State University
210D Mechanical Engineering Bldg.
University Park, PA 16802

Summary

The objective of this effort is to determine the chemical mechanisms of solid propellant ignition and deflagration with an emphasis on the decomposition of individual propellant ingredients and on the gas phase reactions of the products of decomposition. A quadrupole mass spectrometer system using quartz microprobes measures species profiles above the surface of the sample during CO2 laser induced pyrolysis or during laser assisted deflagration of the sample. In addition microthermocouples are used to measure the surface temperature and gas phase temperatures during testing. To complement the experimental studies, chemical kinetic models produced by other researchers are used to model some of the data obtained.

During FY 93, experimental work concentrated on studies of the RDX and ADN. RDX was studied at sub-atmospheric pressures to allow comparison to the results of other researchers and additional work was performed at atmospheric pressure to generate a self consistent data set for modeling. The sub-atmospheric experiments produced results on the initial decomposition of RDX which are generally consistent with the results of other recent studies. In addition one test succeeded in sampling gases from within a bubble on the surface of RDX. The atmospheric testing studies resulted in a self consistent data set for the gas phase species which was then used as the basis for comparison to the results from two different kinetic models. The modeling of RDX results was performed with models by Yetter and Melius. While both models produced good agreement with the measured results, Yetter's model was the better of the two for the conditions of the tests which were modeled.

The ADN study included measurements at pressures above and below one atmosphere and thermocouple measurements of surface and gas phase temperatures. The high pressure tests were performed in an attempt to produce stable flames which could then be probed for species profiles. Unfortunately the flames were not stable enough at five atmospheres, which is the limit of the current system, to permit probing. Analysis of the data from lower pressures for the species leaving the surface of the ADN suggests that two different decomposition paths exist depending upon the experimental conditions chosen. Finally, the thermocouple tests were quite successful and produced consistent values for the surface temperature of the ADN during decomposition of 370K.

After completion of these experimental studies, the mass spectrometer was upgraded to a triple quadrupole to permit identification of species with the same molecular weight but different composition such as CO and N2. This upgrade required substantial re-design of the entire MPMS system as well as the data acquisition and mass spectrometer control software. Also, the CO2 laser underwent a major maintenance to restore its power level to design specifications.

Objective and Approach

The objective of this effort is to determine the chemical mechanisms of solid propellant ignition and deflagration with an emphasis on the decomposition of individual propellant ingredients and on the gas phase reactions of the products of decomposition. The information gained will be coupled into existing modeling efforts supported by ONR. In this program both solid oxidizers and energetic binders will be studied. A quadrupole mass spectrometer system using quartz microprobes is used to measure species profiles above the surface of the sample during CO_2 laser induced pyrolysis or during laser assisted deflagration of the sample. Gas phase temperature profiles are measured with micro-thermocouples no larger than 50 micron. The details of the experimental system used have been described in detail in previous annual reports on this project. (Litzinger)

During the past year a second major objective of the program has been to upgrade the existing single quadrupole mass spectrometer in the microprobe mass spectrometer (MPMS) system to a triple quadrupole mass spectrometer (TQMS). The TQMS will permit the detection and quantification of species with similar molecular weights but different compositions. Several very important species for nitramine propellant combustion such as N_2O and CO_2 at molecular weight 44 and CO and N_2 at molecular weight 28 will be distinguishable with the new TQMS.

Summary of Progress

During FY 93, experimental work concentrated on studies of the RDX at pressures pressures below one atmosphere to allow comparison to the results of other researchers. Work with RDX at one atmosphere also continued with the objective of obtaining a self consistent data set to allow comparison to gas phase kinetic models. Modeling of the RDX results was performed with two models; those of Yetter and Melius (1990). In addition testing of ADN at pressures above one atmosphere was performed to complete the ADN study. Finally the MPMS system was redesigned to incorporate the TQMS and the CO_2 laser underwent maintenance by Coherent to restore its power output. The following sections present more details on the various tasks.

RDX Experimental Studies

Sub-atmospheric Pressure

The laser induced pyrolysis of RDX was studied at a heat flux of 25 W/cm^2 at pressures of 0.1 and 0.5 atm. Laser induced pyrolysis is characterized by the appearance of a shiny liquid layer on the surface of the sample which eventually, and obviously, bubbled with further heating. However, during laser induced pyrolysis, no steady regression of the surface was observed for a typical test duration of two seconds. The lack of steady regression distinguishes laser induced pyrolysis from laser induced regression and laser assisted combustion during which regression of the surface is substantial over a typical test period. Under laser induced pyrolysis the RDX is expected to decompose primarily in the condensed phase; however, near surface gas-phase reactions probably occur. The low pressures and heat fluxes are used to limit the extent of gas phase reactions so that products leaving the surface of the RDX can be measured.

Typical results for this type of test are illustrated by the data in Figure 1. The figure displays the temporal species profiles at approximately 2 mm above an RDX sample undergoing laser induced pyrolysis at a pressure of 0.5 atm. The upper plot indicates species for which calibration was possible and the lower plot gives masses that were detected but not quantified. This particular data set was chosen for discussion because it includes sampling of species from inside a bubble on the surface of RDX.

During this test, laser heating occurred only for the first 3000 milliseconds, but the bubbling continued for some time after laser cut-off. Shortly after laser cut-off, at

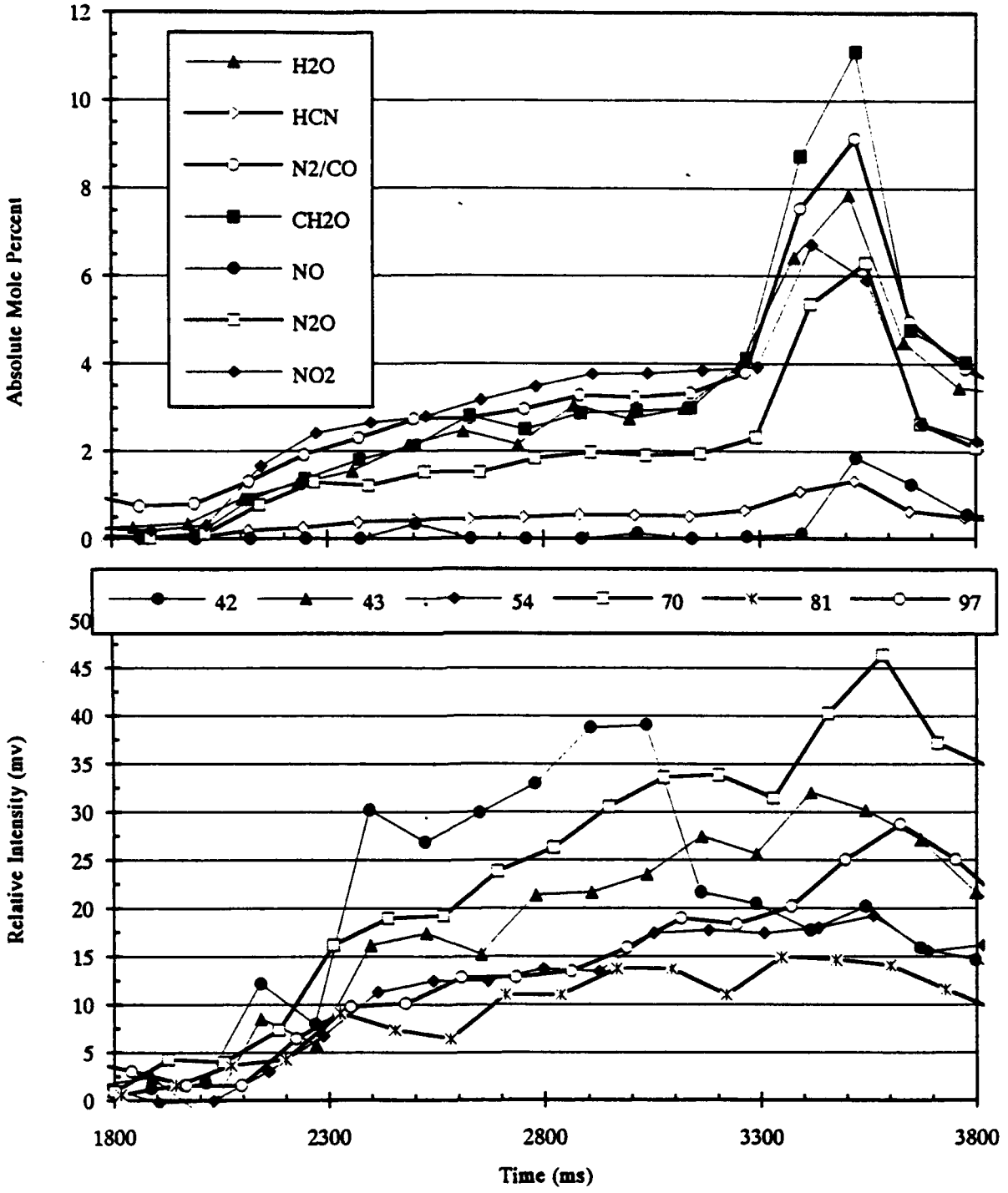

Figure 1. Species profiles for laser induced pyrolysis of RDX at 0.5 atmospheres in argon at a heat flux of 25 W/sq. cm. Laser heating terminated at 3000 milliseconds.

approximately 3300 milliseconds, a large bubble formed which engulfed the tip of the probe and allowed species within the bubble to be sampled. Within the bubble the concentrations of all major species, CH_2O, NO_2, N_2O, H_2O, HCN and NO were larger than outside the bubble due to the lower concentration of diluent argon inside the bubble. However, shifts in relative concentration were also observed. Formaldehyde was the most abundant species inside the bubble, while outside it, NO_2 was most prevalent. These data are the first obtained of species inside a bubble on the surface of an RDX sample and provide important data for modeling the chemical processes in the interior of the bubbles. In contrast to past results for laser assisted combustion of RDX, these pyrolysis results show very low concentrations of NO and HCN above the surface or within the bubble.

The masses plotted in the lower graph are relevant to the initial decomposition of RDX. Even though the test conditions were not equivalent to the very low pressure conditions of Behrens and Bulusu, many of the species they observed, including oxy-s-triazine, a key intermediate product in the decomposition of RDX, were also observed with the MPMS. The oxy-s-triazine intermediate is indicated by the signal at 97 amu, and perhaps by the 70 amu peak which Behrens and Bulusu state is derived from this intermediate. Also found in both studies were the common small gas phase molecules , NO, NO_2, N_2O, H_2O and H_2CO, associated with the decomposition of RDX. Behrens and Bulusu report H_2CN which was not detected in the present study although HCN, which could come directly from H_2CN, was observed.

Some differences did exist between the present work and that of Behrens and Bulusu. Neither the peak at 81 or 43 amu are reported by Behrens and Bulusu. However, Y.T. Lee and co-workers did report signals at 81 amu in their studies using multi-photon dissociation of RDX. During combustion of RDX at 0.5 atmospheres, Korobienichev et al. reported a signal at 43 amu and ascribed it to HNCO. As part of the overall decomposition mechanism for liquid RDX, Behrens and Bulusu report the species NH_2CHO at 45 amu peak which was not detected in the present study.

Atmospheric Pressure

In order to allow modeling of the gas phase chemical reactions above RDX a self consistent data set is required. Here self consistent means that the species must yield atomic species balances which are reasonably consistent with the elemental composition of RDX and also that the temperature of the gas phase near the surface must be

consistent with the enthalpy balance based upon the species measured and the heat of formation of RDX.

The starting point for construction of a self consistent data set is the measured mole fractions for the gas phase species. Because the single quadrupole cannot distinguish CO/N_2 or CO_2/N_2O in a single test, construction of a self consistent data set required multiple test runs. Even with the multiple runs N_2 and CO were not successfully separated so an assumption was made concerning their relative concentrations in order to estimate an atomic species balance for the data. The assumption that was initially made was that N_2 to CO ratio is 1 to 1 throughout the gas phase region based upon the experiments of Korobienichev et al. and the modeling of their data by Melius (1988). The resulting data are shown in Figure 2 along with the atomic species balance. Near the surface of the propellant the element fractions are within 10% of the expected values. However, the upward trend of the C and O element fractions as distance from the surface increases suggests that the assumption concerning N_2 and CO is not correct.

From this point the data set was revised to force the element fractions to balance at the surface of the propellant. This balancing was performed manually using a spreadsheet program and applying the criteria that the smallest possible changes be made from the measured species mole fractions. In order to balance the element fractions at the surface, the N_2/CO ratio at the surface had to be changed to 2 to 1 from the 1 to 1 ratio initially assumed. The balanced species mole fractions at the surface of the propellant and their values from Figure 2 are compared in Table 1.

Once the element fractions were balanced, an enthalpy balance was made to determine the gas phase temperature that corresponded to the resulting, gas-phase species mole fractions. For the test at one atmosphere this temperature was found to be 1075K. This temperature is well above the expected surface temperature of RDX and may be indicative of a near surface reaction zone, first postulated by Korobienichev et al., which cannot be resolved by the MPMS.

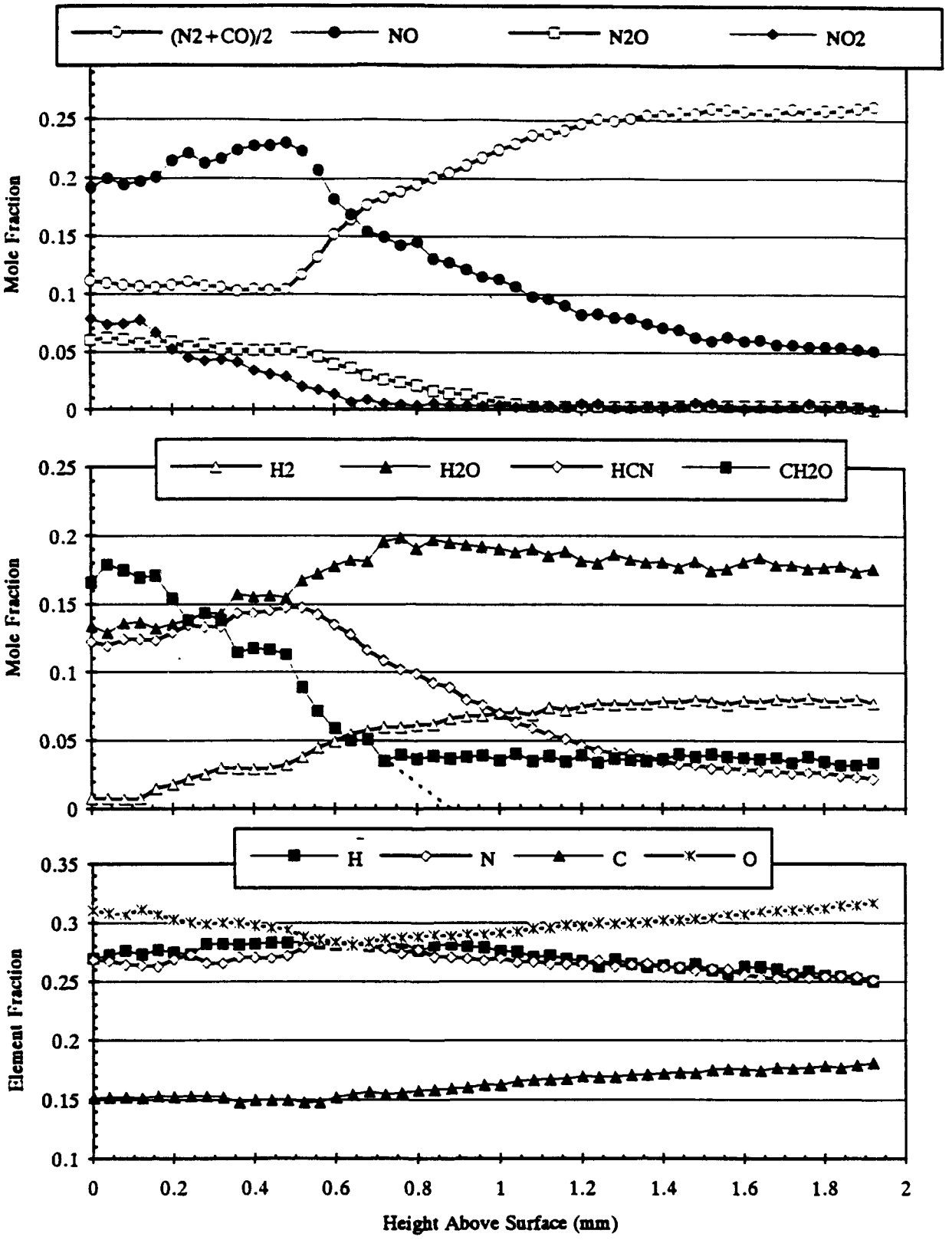

Figure 2. Species profiles for laser induced pyrolysis of RDX at 1 atmosphere in argon at a heat flux of 100 W/sq. cm.

Table 1. Comparison of raw and balanced species mole fractions

Species	Raw Mole Fraction	Balanced Mole Fraction
H2	0.010	0.015
H2O	0.135	0.14
HCN	0.122	0.141
N2	0.11*	0.14
CO	0.11*	0.077
CH2O	0.165	0.17
NO	0.19	0.17
N2O	0.06	0.06
CO2	0.01	0.005
NO2	0.08	0.08

*Based upon assumption that N2 and CO are at equal concentrations

RDX Modeling Studies

In the modeling effort, the self consistent RDX data at 1 atm was used as the basis of comparison to the models of Melius (1990) and Yetter for RDX gas phase chemistry. Both models were run in the Chemkin II PREMIX flame code to predict the gas phase behavior. The initial concentrations of species used were those obtained by balancing the species at the surface of the RDX as described above. Since no temperature profiles have yet been measured for RDX, the temperature profile used in the model was input as a parabolic function with the adiabatic flame temperature reached at the observed flame height and the surface temperature of 1075K set by the enthalpy balance at the surface.

The results in Figure 3 show the predictions of the modeling calculation using the Melius (1990) mechanism and indicate good agreement for most species measured species profiles. However, the disappearance rate of N_2O is too slow and the shapes of the H_2 and H_2O profiles near the surface are not consistent with the measured data in Figure 2. For the results obtained with the Yetter mechanism, presented in Figure 4, the agreement is very good for all species; even the shape of the H_2 and H_2O profiles is well reproduced. One discrepancy remains, however, and that is the distance from the surface to the end of the final flame zone. Although the temperature profile input into the model has the equilibrium reached at approximately 1.8 mm above the surface, reaction in the

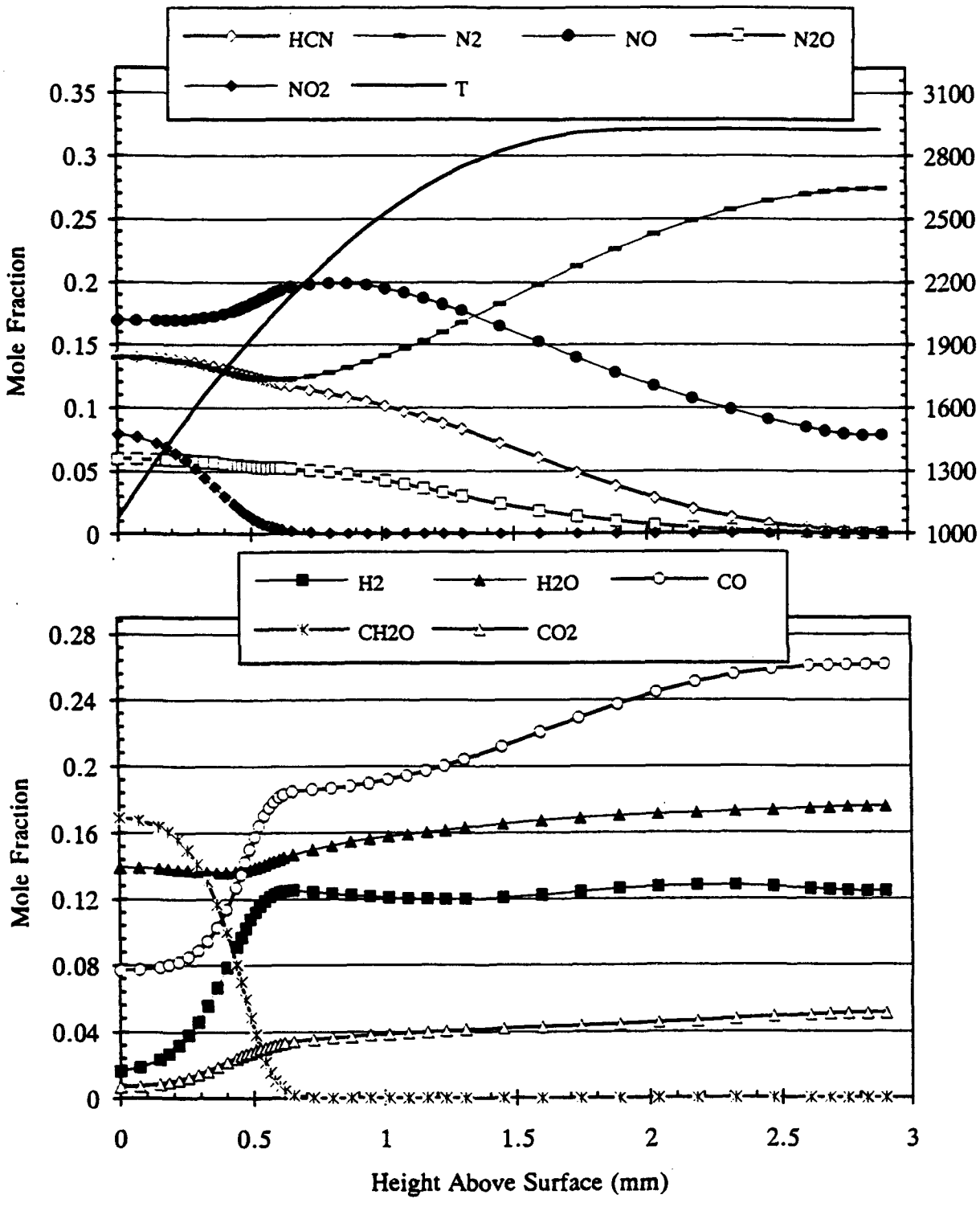

Figure 3. Species profiles generated by 1-D premixed, gas phase flame model of RDX using the kinetic model of Melius (1990).

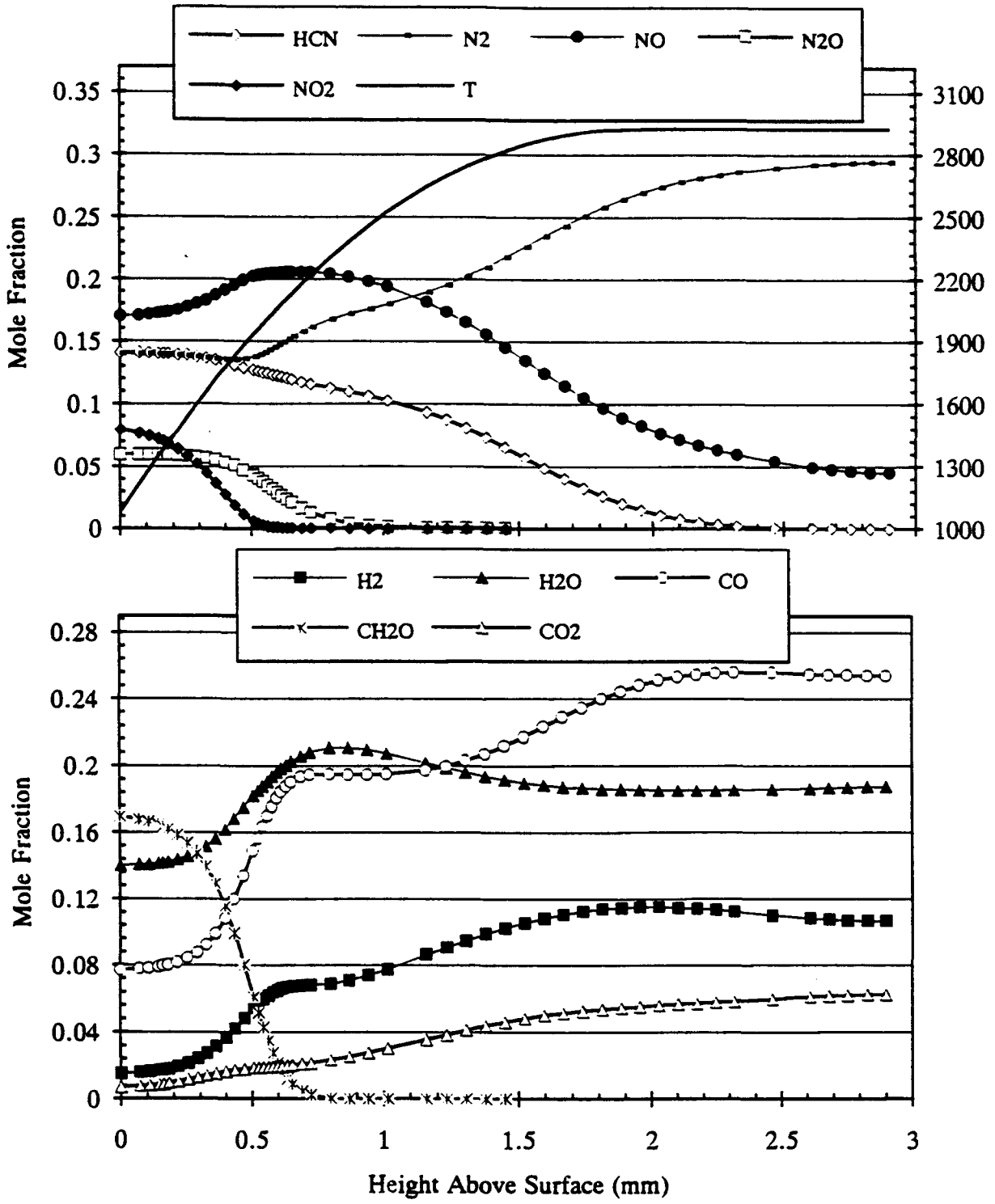

Figure 4. Species profiles generated by 1-D premixed, gas phase flame model of RDX using the kinetic model of Yetter and Dryer.

model continues to approximately 3 mm. A possible explanation for this difference is the energy added by the laser which is expected to be absorbed by the gas phase once ignition has occurred. This additional energy would raise the gas temperature above the adiabatic flame temperature and shorten reaction times and therefore, the lower the height of the final flame. Further studies comparing the models and experiment are required to resolve this difference.

ADN

ADN studies were performed at 5 atm of argon in an attempt to obtain stable flame fronts to allow probing by the MPMS. Increasing the pressure produced more stable flames, but they were not sufficiently one-dimensional to allow probing. Thus these attempts did not produce the desired results. One particular difficulty was the high regression rate of ADN at these conditions, more than five times faster than other materials studied, which resulted in very short test times.

Experiments were also performed at low pressure in an attempt to identify the initial products of decomposition of ADN. Differences in initial products were observed under conditions of slow and fast regression of the surface at low heat fluxes where no flame was present. Under slow regression N_2O was the dominant gas phase product and ammonium nitrate (AN) particles were detected. For fast pyrolysis, NO_2 was detected along with N_2O and H_2O. The products observed were consistent with proposed mechanisms for slow decomposition of ADN into N_2O, NH_3 and HNO_3; the latter species recombine above the surface to form the AN observed. Under fast decomposition, NH_3 and $HN(NO_2)_2$ are the postulated initial products. The $HN(NO_2)_2$ then decomposes to produce NO_2, N_2O and H_2O observed.

Finally thermocouple measurements were made to check the gas phase temperature profile and verify the repeatability of the measurements. Three separate measurements were made, one with Pt/Pt-Rh and two with Chromel/Alumel thermocouples. All test produced very consistent results. Each indicated a rapid rise in temperature, due to the onset of rapid pyrolysis, when the surface achieved a temperature of approximately 370K, near the melting point of ADN. In addition all three tests gave gas phase temperatures near the surface of 750 to 800K. Such temperature measurements can be used to check the self consistency of the species measurements and also provide important information for the testing of chemical models of ADN.

Experimental Facilities

In addition to the work described above, the new MPMS system based on a TQMS was designed and constructed. The upgrade to a TQMS system from the existing single quadrupole MS required substantial revision of the existing MPMS system. The control electronics, the vacuum chamber, the pumping system, the test chamber itself and the test stand were redesigned. In addition, the required characteristics of the TQMS had to be specified to Extrel corporation so that they could begin the construction of the instrument.

All components for the system were received by mid-August when the TQMS was installed by Extrel. The instrument settings are now being optimized for detection and separation of the species of interest. Specifically CO and N_2 being studied because they represent the most difficult pair to separate because of their high bond strengths which will make collisional dissociation difficult. If the optimization and calibration proceed as expected, preliminary experiments with propellants should begin by late October.

In addition to the MPMS modifications, work was done on the CO_2 laser to restore its power output to close to original levels. The work was done by Coherent, the manufacturer of the laser. The necessary repairs included replacement of the unit which recycles the laser gas and repair of a vacuum pump. In addition the laser cavity optics were inspected, cleaned and realigned. In the course of the inspection of the beam delivery system several optical components were found to be damaged and they were replaced.

References

Behrens, R., Jr. and Bulusu, S., *J. Phys. Chem.*, vol. 96, no. 22, pp. 8877-8890 (1992).

Behrens, R., Jr. and Bulusu, S., *J. Phys. Chem.*, vol. 96, no. 22, pp. 8891-8897 (1992).

Korobeinichev, O.P., L.V. Kuiba, V.N. Orlov, A.G. Tereshenko, K.P. Kutsenogii, N.E. Ermolin, V. M. Fomin and I.D. Emel'yanov, *Mass Spektrom. Khem. Kinet.*, pp. *73-93* (1985).

Litzinger, T.A. Final Technical Report, ONR Grant No. N00014-89-J-1238, (1992).

Melius, C. F., Proceedings of the 25th JANNAF Combustion Meeting, CPIA publication 498, Vol.II, pp. 155-162 (1988).

Melius, C.F., Chemistry and Physics of Energetic Materials, edited by S.N. Bulusu, NATO ASI Series, Series C: Mathematical and Physical Sciences - Vol 309, Kluwer Publishers (1990)

Yetter, R.A. and F.L. Dryer, personal communication. (1993)

Zhao, X., E.J. Hintsa and Y.T. Lee, *J. Chem. Phys.*, vol. 88, no. 2, pp. 801-810 (1988).

Appendix

"Chemical Structure of the Gas Phase above Deflagrating RDX: Comparison of Experimental Measurements and Model Predictions"

presented at the 1993 JANNAF Combustion Meeting, Monterey, CA, November 1993.

CHEMICAL STRUCTURE OF THE GAS PHASE ABOVE DEFLAGRATING RDX: COMPARISON OF EXPERIMENTAL MEASUREMENTS AND MODEL PREDICTIONS*

B. L. Fetherolf and T. A. Litzinger
The Pennsylvania State University
University Park, Pennsylvania

ABSTRACT

The physical and chemical processes governing the CO_2 laser-induced pyrolysis and deflagration of RDX were investigated both by experimental studies and kinetic modelling of the gas phase processes. A microprobe/mass spectrometer system was used to measure quantitative gas species profiles and a high-magnification video system was used to record images of the flame structure and surface dynamics. The gas phase processes were modelled as a 1-D, premixed flame with a kinetic mechanism consisting of 31 species and 152 reactions. Tests were conducted at pressures of 0.1, 0.5, 1.0, and 3.0 atmospheres and heat fluxes of 25−1000 W/cm^2. At sub-atmospheric pressures and heat fluxes of 25 W/cm^2, laser-induced pyrolysis (LIP) with stable regression of the surface and no luminous flame was observed which permitted measurement of decomposition species before secondary reactions occurred. Under LIP conditions, the surface exhibited a thick, boiling melt layer with large bubbles. Gas species evolved from the surface and also inside a bubble were measured. CH_2O was found to be the most abundant species within the bubble followed by H_2O, NO_2, N_2O, N_2, and CO. Minor species at molecular weights of 42, 43, 54, 56, 70, 81, and 97 amu were also detected. Species profiles were measured for laser-assisted combustion of RDX at 0.5 and 1.0 atmospheres. A nonluminous primary flame zone produced by the reaction of CH_2O and NO_2 was observed directly above the surface followed immediately by a final luminous flame produced by the reaction of HCN, NO, and to a lesser extent N_2O. The gas-phase chemistry was modelled by using the species measured at the gas-solid interface as input and using a parabolic approximation of the temperature profile. The species profiles generated by the kinetic model were in excellent agreement with the experimental species profiles at one atmosphere.

INTRODUCTION

RDX is a high energy material that has been the subject of numerous studies with a considerable amount of literature published on its decomposition and combustion behavior. However, very few experimental results are available in which gas species above the surface of a deflagrating RDX propellant were measured. The only work which has produced quantitative profiles of all the major stable species is that of Korobeinichev et al.[1] One of the primary objectives of the present work was to measure the complete composition of stable species as a function height above the surface in a similar fashion to the work of Korobeinichev et al. A second objective was to model the gas phase processes with detailed chemical kinetics and to compare the species profiles calculated by the model to those profiles which were experimentally measured. The third and final objective was to measure the decomposition species under laser-induced pyrolysis at low pressures and low heat fluxes to gain some insight into the initial decomposition mechanisms for RDX. Laser energy fluxes of from 20 to 1000 W/cm^2 and pressures of 0.1, 0.5, 1.0, and 3.0 atmospheres were employed for the various experimental studies. All tests were conducted in an argon atmosphere.

EXPERIMENTAL APPROACH

The experimental setup has been described in detail previously[2,3] and a schematic diagram of the sampling configuration is given in another paper presented at this meeting.[4] Only a brief overview of the setup will be given in this paper. The RDX samples were 0.64 cm (0.25") diameter pellets received from Dr. T. Parr of the Naval Air Warfare Center. About thirty tests of RDX pellets were performed. The laser energy source was a CO_2 laser

---

*Approved for public release; distribution is unlimited. This work was performed under ONR Contract No. N00014-93-1-0080 under the sponsorship of the Office of Naval Research, Mechanics Division. The support and encouragement of Dr. R. S. Miller are highly appreciated.

capable of producing 800 watts of continuous wave power. A SONY CCD camcorder fitted with a five-power macro lens was used to record high-magnification color images of the flame structure and sample surface dynamics. This video system permitted relatively precise measurement ($\pm 100\ \mu m$) of probe sampling heights. Gaseous species analysis was performed with a microprobe/mass spectrometer (MPMS) system. The sampling probes were fabricated from 0.32 cm (1/8") quartz tubing and had tip half angles of 10-15° with orifice diameters of 15-25 μm. The experimental control, data acquisition, and data reduction were all performed with a 386-33 IBM PC compatible computer with a high-speed I/O board. For most tests, the MS control program was set to investigate about nine different amu values, i.e., molecular weights, at a sampling speed of 1.5 ms/amu. Various ionization potentials from 14 to 70 eV were used to either minimize fragmentation of the molecules or to separate species at a single molecular weight, e.g., N_2O and CO_2 at 44 amu, by their fragmentation patterns.

The propellant samples were mounted on a spring-loaded sample holder that was attached to a programmable linear positioner inserted through the bottom of a test chamber. The sampling arrangement of the probe with respect to the sample was set up to produce gas sampling along a central axis normal to the sample surface.[4] For all species profiling tests, the probe was initially positioned above the reaction zones and the sample was moved upward by the linear positioner at a rate slightly faster than the regression rate until the surface contacted the probe. The MPMS system was calibrated before each day of testing so that quantitative species profiles for the stable gas species products could be determined. Water vapor and formaldehyde were calibrated by heating a small cup of liquid water or formaldehyde solution under the probe with the CO_2 laser. The gas composition as a function of the height above the surface was reported as "normalized" mole fractions by adding the measured concentrations of the measured species together and dividing each concentration by this total. This method was also employed by Korobeinichev et al.[1] Normalizing the mole fractions with this approach cancelled out the effect of sample temperature on the observed signal intensities and also cancelled out any effect of signal reduction by probe orifice constriction during a test.

KINETIC MODELLING

The overall objective of the kinetic modelling was to develop a detailed model of the gas phase chemistry occurring during RDX combustion. Specifically, the model was used to generate gaseous species profiles as a function of the height above the material surface which could be compared directly to the experimentally determined species profiles. The gas phase was modelled as a quasi-one-dimensional, laminar, steady flow of a premixed gas mixture at constant pressure. The model was solved with the CHEMKIN II software package[5-7] and the PREMIX subroutine.[8] Melius[9] has used the same general approach of assuming a premixed flame for his model of RDX combustion and also used the CHEMKIN software to solve the model. Melius considered the condensed phase in the model by treating it as a "pseudo gas" with the physical properties of the solid and by adding a single-step condensed-phase decomposition mechanism. Ermolin et al.[10] have also used the 1-D, premixed flame approach to model RDX combustion but modelled only the gas phase by using the gas composition right at the gas−solid interface which was measured experimentally[1] as part of the initial conditions. The latter approach was also used in the kinetic modelling work presented in this paper.

The PREMIX subroutine required as input the mass flux from the surface and the temperature profile if the energy equation is not to be solved by the model, the approach that was used in the present work. The mass flux can be calculated by doing a mass flux balance at the surface if the burning rate is known. Burning rates were measured by post-test analysis of the video recordings for each experiment. The temperature profiles could not be measured with fine-wire Pt−Pt/13%Rh thermocouples because of the high flame temperature. Thus, a profile was assumed based on a parabolic approximation of the temperature from the initial gas temperature to the final flame temperature. This will be discussed further in the Results and Discussion.

The kinetic mechanism of Yetter and Dryer[11] was employed as the elementary reaction scheme for the model. Their mechanism[11] contained decomposition reactions for the parent RDX molecule and reactions for the larger RDX fragments such as methylene nitramine. Since these species were not measured with the MPMS system, they were not included in the mechanism for the present model. Only the species measured at the surface and all radical or intermediate species believed to participate in the subsequent reaction scheme were included. The highest molecular weight species included in the model was NO_2. The final mechanism used for the modelling efforts consisted of 31 species and 152 reactions.

RESULTS AND DISCUSSION

The experimental results will be presented and discussed in two different sections, each section representing a distinctly different category of laser-induced behavior. The first section denoted "Laser-induced Pyrolysis" (LIR) discusses tests where the sample was pyrolyzed by the laser energy and the sample surface simply pyrolyzed, melted, and bubbled and did not exhibit any quasi-steady regression of the surface. The second category was "Laser-assisted Combustion" (LAC) where the surface regressed stably with a luminous flame observed above the surface. The results for kinetic modelling of RDX combustion will be presented in a third section.

The results that will be presented here are graphs of gas species and temperature profiles as a function of the height x above the surface for LAC conditions and or as a function of time for LIP conditions. The gas composition was quantified in terms of the species mole fractions (X_i) as described in the Experimental Approach. Both element and enthalpy conservation were employed in the analysis of the gas species composition data. Fristrom and Westenberg[12] provide an excellent discussion of the analysis of experimental flame data which includes the use of element and enthalpy conservation equations in the analysis. The following element conservation equation was employed in the present study to obtain the element fractions Z of each element j as a function of the sampling height x above the surface:

$$\sum_{i=1}^{N} \nu_{j,i} X_i(x) = Z_j(x) \tag{1}$$

where $\nu_{j,i}$ is the number of atoms of element j in species i and X_i is the mole fraction of species i for the N species measured. Obviously, the element fractions obtained with equation (1) should correspond to the fractions of each element in the original material. Equation (1) neglects the effects of species diffusion which may not be negligible in regions of strong concentration gradients as will be addressed when discussing the results. Enthalpy balances at a certain location above the surface were performed using the following equation:

$$\sum_{i=1}^{N} X_i H_i(T) = X_o \Delta H_{f,o} \tag{2}$$

The left side of equation (2) sums the enthalpies of the N gas species measured as a function of temperature $H_i(T)$ where the enthalpies were calculated using the thermodynamic database in the CHEMKIN software.[6] The right side of equation (2) represents the enthalpy content of the original material where X_o is calculated by writing an overall reaction for the breakdown of the original material into the measured gas composition. The fraction of the original material required to balance the overall reaction with respect to the element content in the gases then defines X_o. As with the element balance in equation (1), equation (2) is only valid in "equilibrium" regions above the surface, i.e., where no large gradients in species or temperature exist. The validity of using this equation will be discussed further when it is applied.

LASER-INDUCED PYROLYSIS

Laser-induced pyrolysis (LIP) of RDX was observed for tests at low pressures of 0.1 or 0.5 atmospheres of argon with a low incident heat flux of 25 W/cm^2. The first distinct and continuous sign of the onset of pyrolysis was melting of the surface. Admittedly, the term "melting" is used loosely in this discussion. Boggs[13] noted that several researchers question whether the liquid layer on the surface was produced by a true melting phenomenon or by dynamic breakup of the RDX crystal lattice accompanied by chemical decomposition. The heterogeneity of the mixture of decomposition products and parent RDX molecules may cause liquefaction of the surface material. The visual evidence of melting in this study was dynamic motion of the surface and the appearance of a glossy liquid layer on the surface. The dynamic motion was seen as both a slight upward expansion of the surface and random boiling motion. The expansion was due to a slight change in density as the material melted and also due in part to the evolution of subsurface gases due to decomposition occurring immediately after the onset of liquefaction. Behrens and Bulusu[14] stated that they observed significant quantities of gaseous decomposition products as soon as RDX started to liquefy at 198°C.

Figure 1 displays temporal species profiles for gas sampling about 2.0 mm above an RDX sample surface under LIP conditions. The upper graph in Figure 1 displays profiles for the calibrated species in absolute mole percent, i.e., without normalizing the concentrations to obtain mole fractions. The lower graph in Figure 1 gives profiles for species at certain m/e values in the form of relative intensities, i.e., signal strengths in millivolts, since the species in these graphs were not calibrated. The incident heat flux was 25 W/cm^2 and the pressure was 0.5 atmospheres. Laser heating was terminated at three seconds. The mass spectrometer was set to ramp at 1.5 ms/amu from 15 to 100 amu with an ionizer potential of 22 eV to acquire the data displayed in Figure 1.

The video images for the test displayed in Figure 1 showed that the surface melt layer boiled vigorously with no luminous emission. The boiling phenomenon became more subdued after the laser heating was terminated but still continued to some extent for several more seconds. Liquid material and bubbles growing from the surface layer reached a height of roughly one millimeter during laser heating. However, after laser heating was terminated, a very large bubble formed at the surface and expanded to encompass several millimeters of the probe tip. The result of this phenomenon was gas sampling within the bubble of decomposition gases evolved from the RDX surface evidenced by the rise in several species profiles between 3300 and 3700 milliseconds in Figure 1. Formaldehyde was the most abundant gas within the bubble followed by N_2 and CO, H_2O, NO_2, and N_2O. Only a small amount of HCN was observed either above the boiling surface or within the bubble. Nitric oxide (NO) was not observed above the pyrolyzing surface except for a small amount at 2500 milliseconds. A small amount of NO was also observed to develop late in the formation of the bubble. It is interesting to note the very small amount of HCN and NO both in the bubble and above the surface under these conditions. Considerable amounts of both these species (>0.12 mole fraction) were observed directly above the surface under LAC conditions for RDX as will be discussed in the next section. It was also of interest that NO_2 was found to be the most abundant species above the surface but was less abundant within the bubble than CH_2O, H_2O, and species at 28 amu (N_2 and CO). This may imply that there are other species within the bubble that decompose or react to produce the NO_2 observed above the surface.

The lower graph in Figure 1 provides intriguing evidence of the less common species observed in the RDX decomposition spectrum. The production of the species at 42 amu appeared to be driven by the external energy input. Both Schroeder[15] and Farber and Srivastava[16] list the structure of the species at 42 amu as $CH_2NCH_2^+$, a radical that would not be detected by the MPMS system. However, Behrens and Bulusu[14,17] found in their studies that the signal at 42 amu originated from ONDNTA at 206 amu and also observed the abundance of ONDNTA to rise gradually as the sample temperature increased between 195°C and 215°C. It was likely that the melt layer temperature for the test in Figure 1 also rose gradually after the onset of gas evolution during which time the abundance of the species at 42 amu was observed to increase until laser heating was terminated. The similarity of the 42 amu profile and the temporal behavior of ONDNTA in the tests by Behrens and Bulusu may provide evidence of ONDNTA formation in the test depicted in Figure 1.

The species characterized by the 43 amu profile in Figure 1 was believed to be HNCO. This species has what appears to be a stable structure (H=N–C=O) from a simple electron structure balance and should thus be detectable by the MPMS system. Interestingly, Behrens and Bulusu,[14,17] Farber and Srivastava[16], and Zhao et al.[18] make no mention of this species even as a fragment of other larger species. Goshgarian[19] listed two structures for a species at 43 amu but gave no profiles for this species. Korobeinichev et al.[1] observed HNCO as a rapidly decaying profile near the surface. The studies in references 14 and 16–19 were all conducted at pressures several orders of magnitude lower than the pressure of 0.5 atmospheres employed by Korobeinichev et al.[1] and used in the present study (see Figure 1). Goshgarian[19] observed lower molecular weight species to be dominant for his atmospheric pressures tests while higher molecular weight products became more important under high vacuum (10^{-7} torr). Oyumi and Brill[20] have also observed HNCO in their thermolysis studies of RDX. It is thus postulated that different chemical mechanisms may occur at very low pressures which do not form HNCO but that the mechanisms at pressures approaching atmospheric pressure may favor the formation of a small amount of HNCO.

Small signals at m/e values of 54 and 56 (not pictured in Figure 1) were also observed. The 54 amu signal showed no dependence on sampling within the gas bubble in Figure 1. A proposed stable molecular structure for the species at 54 amu could be H_2CNCN which may be produced directly from the RDX ring with the NO_2 groups stripped from the ring nitrogens and the one carbon atom being stripped of its hydrogens. However, the inner

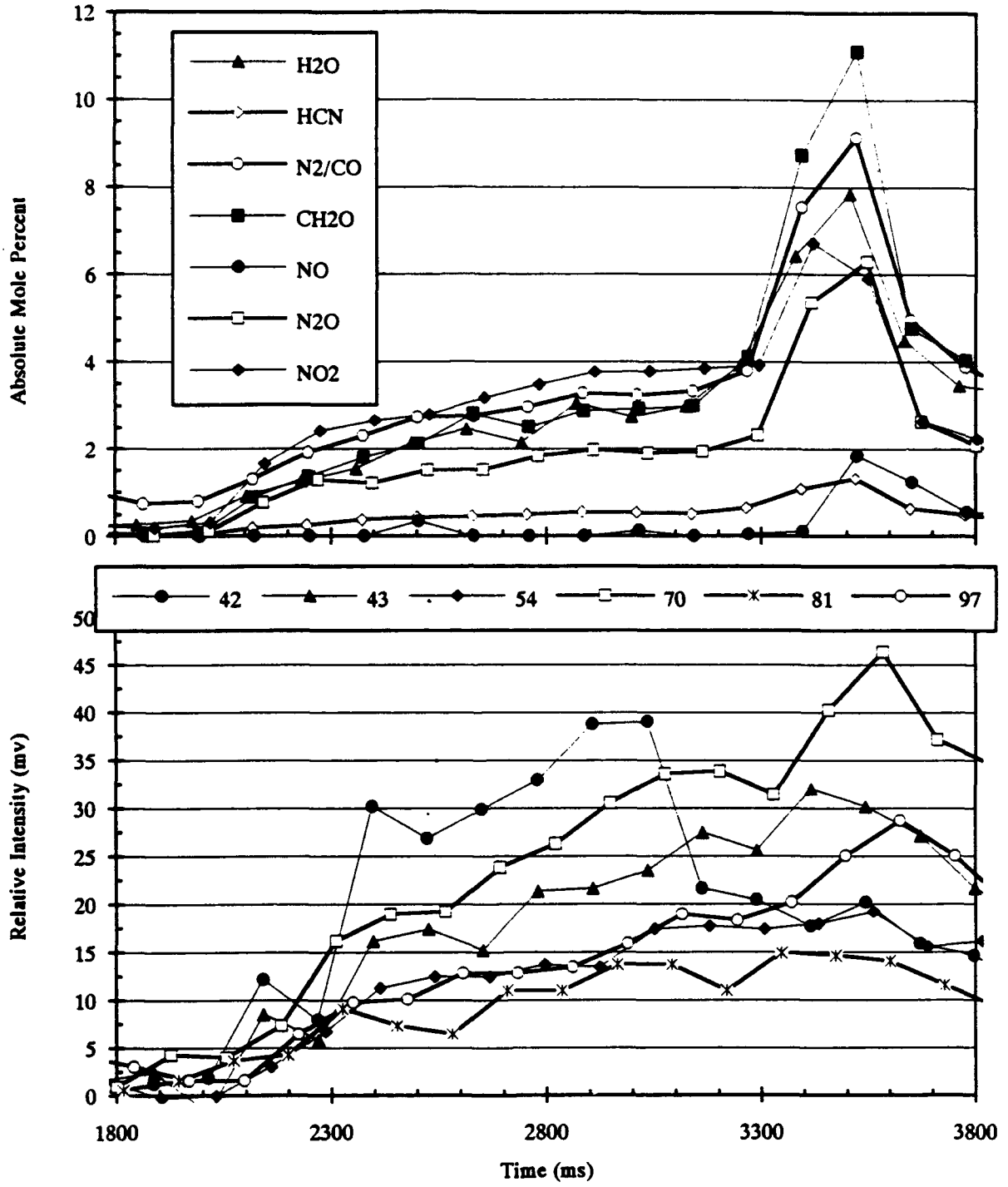

Figure 1. Species measurements for pyrolysis of RDX at 0.5 atmospheres in argon with a heat flux of 25 W/sq cm. Laser heating was terminated at 3 seconds. The sampling height was 2.0 mm. The numbers in the lower chart are species molecular weights.

nitrogen would have to form a double bond with the left carbon while the end nitrogen would have to form a triple bond with the carbon next to it in order for the molecule to be stable. A structure for the 56 amu molecule given in references 13 and 15 was $HNCHNCH_2$, a structure which again could be produced directly from the RDX ring structure.

Behrens and Bulusu stated that the species they observed at 70 amu originated from the species at 97 amu. The rough temporal correlation of these species in Figure 1 appeared to substantiate that the 70 and 97 amu peaks were not independent of one another. A test was conducting at a lower ionizer potential of 17 eV and at 0.1 atmospheres to investigate whether the 70 peak would again correlate to the 97 peak profile and greatly diminish in intensity, suggesting that it was merely a fragment produced by the MS ionizer. For the test at the lower Ev, the 70 and 97 amu profiles displayed distinctly different trends and after laser heating was terminated, the 97 amu profile went almost to zero while the 70 amu profile maintained a significant intensity. Thus, the species at 70 amu was believed to be a distinct decomposition species. Two molecular structures for the species at 70 amu which were not linear in structure were given in references 13 and 15. Goshgarian[19] observed the amount of a species at 70 amu to increase during melting for RDX, in agreement with the trends depicted in Figure 1.

The species at a molecular weight of 81 amu has also been observed by Zhao et al.[18] and Goshgarian[19] who both proposed a structure for this molecule where the original ring structure for RDX remained intact but all the NO_2 groups and three of the H atoms were removed from the ring structure. Fifer[21] offered a scheme whereby the structure of this species was arrived at by successive elimination of three HONO molecules. Fifer then proposed that the 81 amu species may decompose to form three HCN molecules. Figure 1 indicates that the profile for this species at 81 amu was unaffected by sampling in the gas bubble from 3300-3600 milliseconds.

To the author's knowledge, the only other studies identifying a species at 97 amu are those by Behrens and Bulusu[14,17] and Snyder et al.[22] which was referenced by Behrens and Bulusu. Behrens and Bulusu[14] list three possible structures for this molecule and label it as oxy-s-triazine (OST). Farber and Srivastava[16] did not observe OST under conditions similar to those of Behrens and Bulusu. The fact that Zhao et al.[18] did not observe OST in their IRMPD analysis of individual RDX molecules may imply that OST is produced by reactions within the heated bulk material. Figure 1 shows a slowly rising profile for OST with a distinct rise during probe sampling in the bubble.

Interestingly, no distinct peaks were observed for any species with a molecular weight above 97 in the present study even though the mass spectrometer was ramped up to 224 amu for the test at the lower eV and pressure setting. Behrens and Bulusu[14,17] and Farber and Srivastava[16] have detected several species with molecular weights greater than 100 in slow heating rate tests and Zhao et al.[18] also detected species of this size in their IRMPD experiments. It is hypothesized that the lack of observation of any species with molecular weights above 100 in the present study may be attributable to a difference in the decomposition mechanisms between the high heating rate and near atmospheric pressure studies of the present work and the slow heating tests[14,16,17] and IRMPD experiments[18] conducted at very low pressures.

LASER-ASSISTED COMBUSTION

Many tests of RDX characterized as laser-assisted combustion (LAC) were conducted at pressures of 0.5 and 1.0 atmospheres of argon with one test also performed at 3.0 atmospheres. The heat flux was varied from 50−1000 W/cm^2. Video recordings of flame heights and regression rates as a function of pressure and heat flux were obtained. Gas species profiles were measured by strategically planning the positioner movement control sequence so that the probe tip spent very little time in the hot final flame. It was found that at these test pressures the probe tip could not be located in the hot flame for more than about 300 milliseconds without the orifice melting shut.

The onset of the luminous flame was very abrupt with the flame appearing almost instantaneously at roughly a steady state height above the sample surface and remaining quite stable there until the laser heating was removed. A thin violet flame zone separated from the surface by a nonluminous zone was observed with a sizable deep yellow flame above the violet flame. The location of the violet flame zone above the surface was strongly dependent on both pressure and incident heat flux. The flame exhibited a slight dome shape due to both the nonuniformity of the

laser beam profile and edge effects commonly observed for combustion of small propellant samples. At one atmosphere, it was previously determined[3] that the critical heat flux for establishment of a luminous flame was 43 ± 5 W/cm^2. At 0.5 atmospheres, the critical heat flux was roughly 100 W/cm^2. But even at this heat flux level, a substantial delay to the appearance of the flame of greater than one second was usually observed. During this delay, the surface boiled profusely. The fact that any flame developed after such a substantial delay may be evidence of autocatalytic effects and/or buildup of certain combustion-initiating species in the surface melt layer. The height of the thin violet flame zone at 0.5 atmospheres and 100 W/cm^2 was roughly $2.0-2.5$ millimeters. When the pressure was raised to one atmosphere with the same heat flux, the flame height dropped to about 0.6 millimeters. At one atmosphere and a heat flux of 1000 W/cm^2, the flame height was about 5.0 millimeters. A test run at three atmospheres and 100 W/cm^2 showed that the flame zone collapsed to very close to the surface (<200 μm) with a barely distinguishable nonluminous region between the zone and the surface.

Figure 2 displays species profiles and element balances for a test of RDX at one atmosphere in argon with a heat flux of 100 W/cm^2. Preliminary results given previously[3] were expanded upon to produce the results given in Figure 2. These results represent a compilation of several different tests conducted at different eV settings and with different positioner movement programs to obtain species profiles through the various zones in the gas phase before the quartz probe melted, an event that happened more often than not at this pressure. Tests were run at eV settings of 15.5 eV (roughly the appearance potential of CO_2), 22 eV, and 40 eV to try to separate CO_2 and N_2O at 44 amu and CO and N_2 at 28 amu. N_2O and CO_2 were resolved and are depicted in Figure 2. However, difficulties were encountered in resolving CO and N_2 at 28 amu. The species profiles for deflagration of RDX at 0.5 atmospheres measured by Korobeinichev et al.[1] and calculated by Melius[9] indicate that N_2 and CO are of roughly the same concentration from the propellant surface through the final flame for RDX. Thus, as a first approximation, the signal at 28 amu was assumed to be equally due to CO and N_2 throughout the gas phase.

Figure 2 indicates that the primary flame zone reactions began to accelerate about $150-200$ μm above the sample surface evidenced primarily by the consumption of CH_2O and NO_2. This reaction has been proposed by several researchers to be the dominant reaction in the primary flame for RDX. Interestingly, Korobeinichev et al.[1] did not observe any formaldehyde in their tests of RDX. A significant amount of CH_2O above the surface of deflagrating RDX-based propellants has also been reported.[4] The level profile of formaldehyde after 0.7 mm was not a common observation for RDX tests under these conditions as noted by the "expected trend" line drawn down to zero at about 0.85 millimeters. A possible reason for this anomalous CH_2O profile was the condensation of some of the sampled formaldehyde on the inside of the probe or the MPMS vacuum chambers with subsequent evaporation producing the level CH_2O profile. The secondary flame zone characterized by the thin violet flame began at a height of about 550 μm. At this location, the primary flame reaction was not quite completed with NO_2 fully consumed at about 650 μm and the CH_2O profile leveling off at 700 μm. N_2O remained relatively inert through the primary flame and was consumed in the secondary flame. About 0.03 and 0.04 mole fraction of HCN and NO, respectively, were produced in the primary flame zone. In the secondary flame, NO and HCN were consumed at about the same rate, consistent with reduction of NO by HCN being the primary reaction in the luminous flame zone as noted by Korobeinichev et al.[1] Small amounts of CO_2, H_2, and H_2O and substantial amounts of CO and N_2 were produced by the reactions in the luminous flame.

The bottom graph in Figure 2 displays the element fractions for the species profiles. The original element fractions in RDX are 0.286 for H, N, and O and 0.143 for C. The measured element fractions at the surface are 5% and 8% high for C and O, respectively, and about 5.5% low for H and N. The excess of C and O and shortage of N may indicate that there is more N_2 than CO at the surface instead of the assumption of equal amounts used in deriving the element fractions portrayed in Figure 2. This may also be the case in the final flame since all species are almost perfectly conserved at a height of 550 μm but the amount of C and O continuously increase above this height. The amount of H is poorly conserved as the profiles approach the final flame and is 12% low at the end of the profile. This may be due to slight errors in the calibration factors for H_2 and H_2O, both of which were somewhat difficult to calibrate. Balanced element fractions will be presented in Table 1.

Species profiles for deflagration of RDX at 0.5 atmospheres with a heat flux of 150 W/cm^2 are displayed in Figure 3. About eight tests were conducted at this pressure with heat fluxes between 100 and 200 W/cm^2. Some difficulties were encountered in attempting to measure profiles from the surface through the flame zone primarily

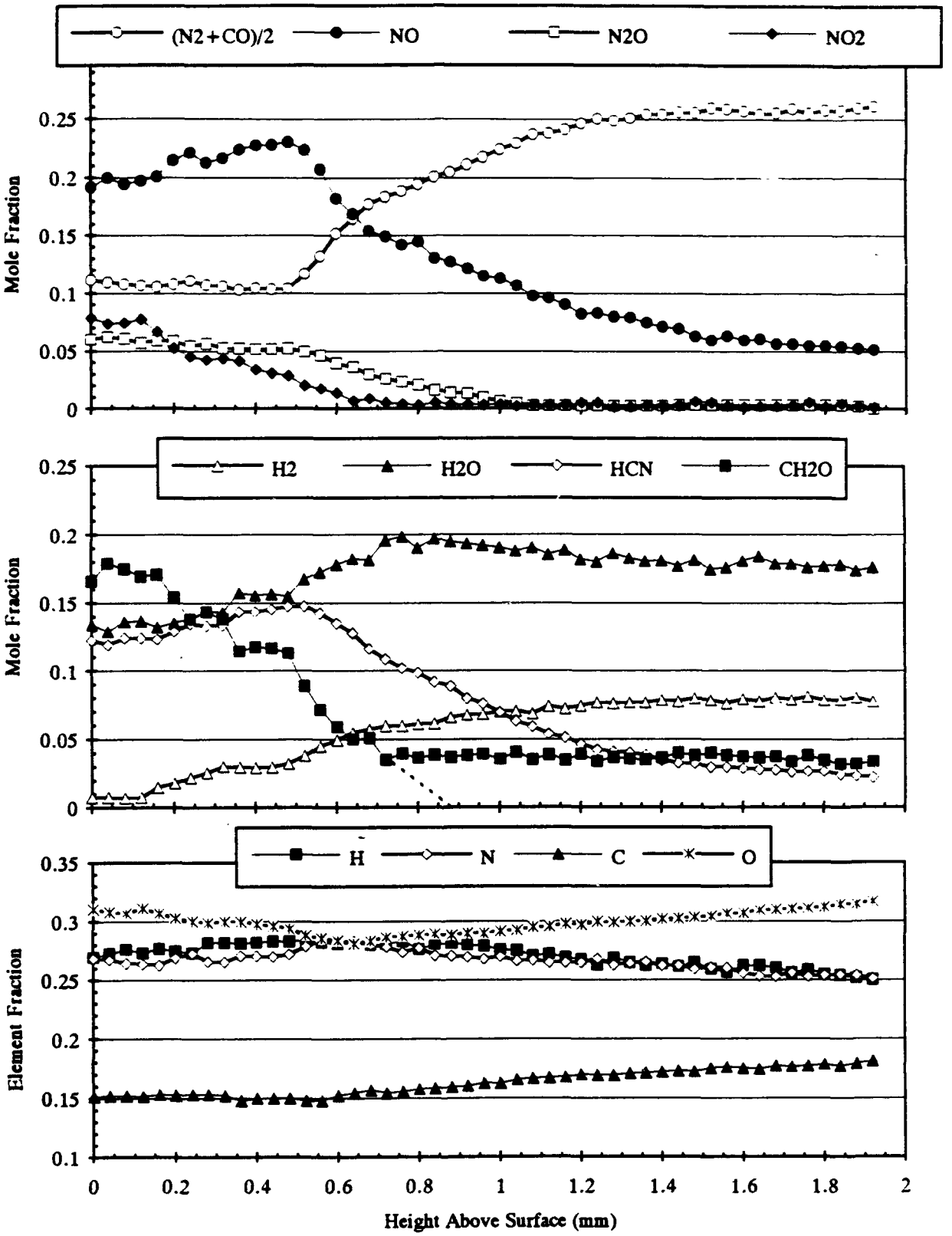

Figure 2. Laser-assisted combustion of RDX at a pressure of one atm. in argon with a heat flux of 100 W/sq cm

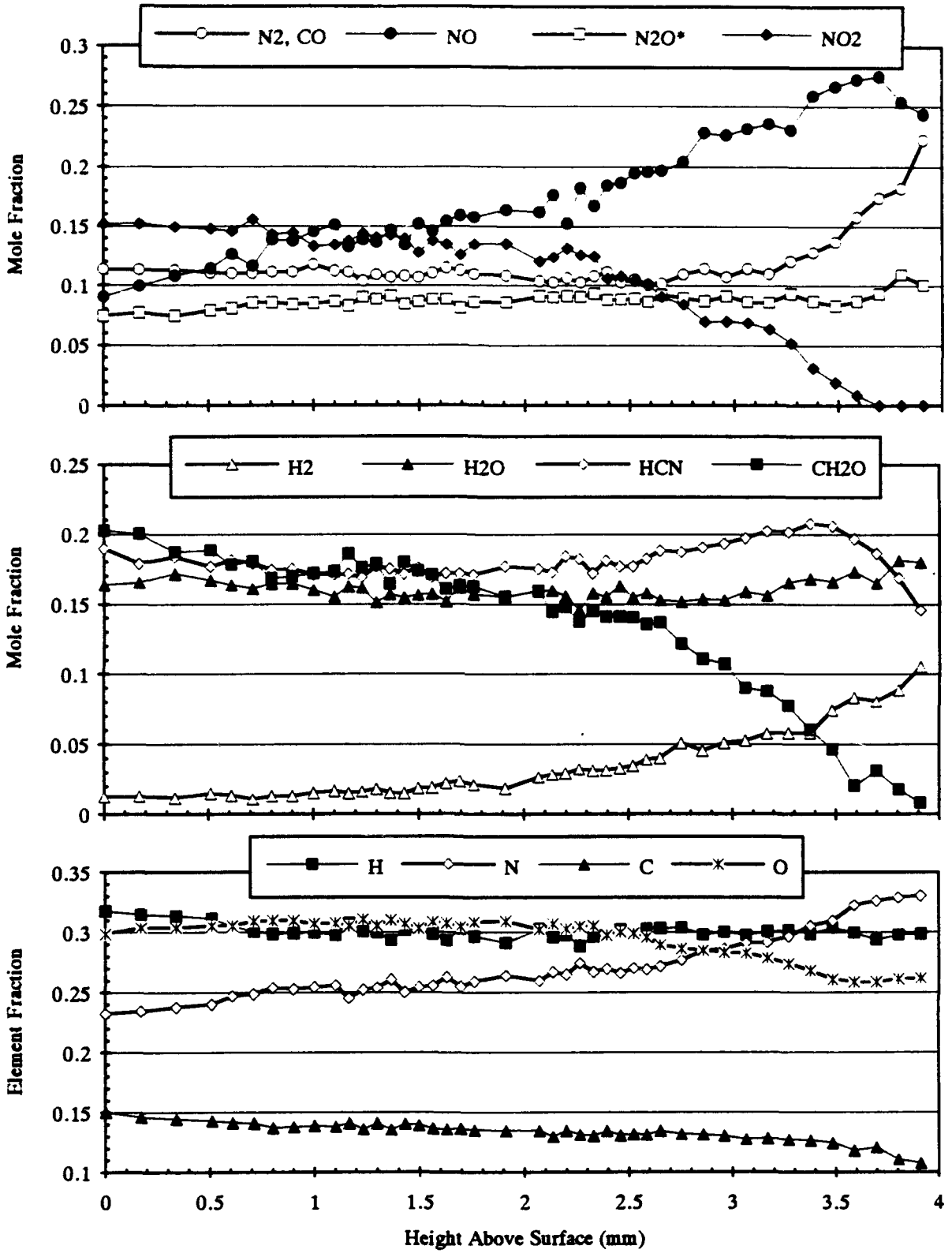

Figure 3. Laser-assisted combustion of RDX at a pressure of 0.5 atmospheres in argon with a heat flux of 150 W/sq cm. *The N2O profile was derived by assuming the signal at 44 amu was totally due to N2O.

due to the instability of the flame at the lower pressures. The standard procedure for obtaining species profiles was to start with the initial sampling height set slightly higher than the expected flame zone location and then move the sample toward the probe when combustion started in such a way as to keep the probe in the flame for no more than about 300 milliseconds. But, when the probe was set this close to the flame at this pressure, the flame tended to "overshoot" its steady state location and attach to the probe for a short period of time before settling down to a quasi-steady position. If the probe was set at a higher initial height to avoid the flame attachment, it would be melted before it passed through the flame into the cooler region. The profiles in Figure 3 represent the best effort at defining the point of onset of the final flame reactions but do not reveal the final post-flame gas composition. The height of the onset of the final flame seen in Figure 3 is quite a bit farther from the surface than the steady state location due to sampling during the initial overshoot of the flame. The steady state location was roughly 2.0−2.5 millimeters above the surface. The stretching of the spatial scale of the profiles was not believed to alter the chemistry and from an analysis standpoint was helpful because it increased the spatial resolution.

The profiles in Figure 3 exhibit the same overall zonal structure leading up to the final flame as was observed at one atmosphere (see Figure 2) with the CH_2O/NO_2 reaction dominating the primary flame. The zonal structure inferred from the profiles in Figures 2 and 3 does not reveal a levelling off of the species profiles characteristic of a "dark zone." The experimental results of Korobeinichev et al.[1] also gave no evidence of a dark zone. The overall difficulties encountered in running the tests at 0.5 atmospheres precluded the resolution of the species at both m/e values of 28 and 44. For Figure 3, the profile at 44 amu was assumed to be N_2O throughout and the 28 amu signal was again assumed to be equally due to CO and N_2. The most significant difference in species concentrations observed in Figure 3 in comparison to Figure 2 was a factor of two increase in the mole fraction of NO_2 (X_{NO2}) at the surface and the same factor of decrease in X_{NO}. The profiles for NO and NO_2 appear to be intimately coupled in Figure 3 as NO is produced at roughly the same rate as NO_2 is consumed. Oyumi and Brill[20] also observed this NO/NO_2 coupling for RDX. The total of CO and N_2 at the surface was one half of the CO/N_2 total observed at one atmosphere. Figure 3 indicates a very low element fraction of N at the surface, possibly implying that the signal at 28 amu should be attributed mostly to N_2 as it was for the profiles in Figure 2.

Table 1 lists gas compositions and temperatures calculated from enthalpy balances using equation (2) at both 0.5 and 1.0 atmospheres. Results are given for the work in the present study (Figures 2 and 3), the work by Korobeinichev et al.,[1] and the results of calculations of the final gas composition using the NASA-Lewis equilibrium code[23]. The notation of "balanced" or "unbalanced" refers to whether the element fractions for that reference were fully conserved. The "balanced" references for the present study were derived by taking the actual measured data at the surface from Figures 2 and 3 and manually forcing a balance. This was done with a simple spreadsheet program by making small changes in the appropriate species mole fractions until all the element fractions were exactly balanced to the same fractions found in the original material. This approach was used simply as a first approximation since there were more equations than unknowns to properly balance the gas composition. The most important consideration when doing this manual balance was to keep the species mole fractions as close as possible to those experimentally measured. After the element fractions were balanced, an enthalpy balance on the resultant species composition was performed using equation (2) to derive the temperatures given in Table 1. Using equations (1) and (2) require that species diffusion and heat conduction both be negligible in the region of interest. The magnitude of the diffusive flux is based on the concentration gradient for each species (dX_i/dx) and the conductive heat flux depends on the temperature gradient (dT/dx). The species profiles in Figures 2 and 3 display little or no gradient in concentration at the gas-solid interface which validates the assumption of negligible diffusion effects at this location. Since there were no significant concentration gradients in species, it would be expected that any temperature gradient at the surface would not be large either. Thus, the conductive heat flux to the surface should also be negligible, and the use of equation (2) should also be considered a valid approach.

To achieve an element balance for N at the gas-solid interface for the test at one atmosphere, the signal at 28 amu had to be divided such that the fraction of N_2 was twice that of CO instead of the equal balance previously assumed. This resulted in a gas-solid interface temperature of 1075 K. The balancing of the raw data at the interface for the test at 0.5 atmospheres (Figure 3) required some rather significant changes in several mole fractions with 11-18% changes in H_2O, CH_2O, NO, and NO_2 to produce a balance. The signal at 28 amu had to be increased about 40% to produce enough N_2 to bring the N fraction into balance. Thus, there was less confidence in the gas composition measured at the gas-solid interface for Figure 3 than for the data given in Figure 2. The calculated

Table 1. Comparison of gas species compositions and calculated temperatures at various pressures and locations for the present study , the work of Korobeinichev et al.,[1] and equilibrium code[23] calculations

Region of Interest - Reference	P (atm)	T (K)	Species										
			H2	H2O	HCN	N2	CO	CH2O	NO	N2O	CO2	NO2	HNCO
Composition at Surface													
- Present Study (balanced)	1	1075	0.015	0.14	0.141	0.14	0.077	0.17	0.17	0.06	0.007	0.08	0
- Present Study (balanced)	0.5	936	0.005	0.145	0.187	0.12	0.043	0.17	0.11	0.08	0.01	0.13	0
- Korobeinichev et al.	0.5	1308	0	0.238	0.244	0.078	0.044	0	0.238	0.044	0.069	0.024	0.024
Post-Flame Region													
- Present Study (raw data)	1	-----	0.0776	0.176	0.022	0.2613	0.261	0	0.0514	0	0.1143	0	0
- Present Study (balanced)	1	3187	0.112	0.218	0	0.315	0.24	0	0.03	0	0.086	0	0
- Present Study (balanced)	0.5	3397	0.103	0.225	0.015	0.323	0.208	0	0.013	0	0.113	0	0
- Korobeinichev et al.	0.5	-----	0.113	0.257	0	0.231	0.256	0	0.03	0	0.113	0	0
Post-Flame Region					H			O		O2			OH
- Equilibrium Code	0.5	2858	0.091	0.191	0.042	0.314	0.243	0.008	0.004	0.007	0.073	0	0.027
- Equilibrium Code	1	2925	0.091	0.196	0.037	0.316	0.244	0.006	0.004	0.006	0.074	0	0.026
- Equil. Code w/o Radicals	1	3274	0.0977	0.211	0	0.3394	0.2621	0	0.0043	0.006	0.0795	0	0

gas-solid interface temperatures for the experimental data were far above the "surface reaction zone" temperature of 620-670 K proposed by Brill et al.[24] The gas composition measured by Korobeinichev et al.[1] at the gas-solid interface (see Table 1) was almost perfectly balanced with respect to the element fractions, but an enthalpy balance produced a high gas temperature of 1308 K. Korobeinichev et al.[1] and Ermolin et al.[10] both stated that this high gas-solid interface temperature confirmed the existence of a very thin decomposition zone just above the surface which they could not resolve with their sampling probe. Korobeinichev et al. believed that this zone was due to the rapid decomposition of gaseous RDX evolved from the surface. The results of the present study appear to confirm the hypothesis of a thin reaction zone directly above the surface. However, it is also postulated that much of the RDX may decompose in a heterogeneous melt layer, i.e., in gas bubbles in the melt layer which were observed under LIP conditions. The RDX decomposition species, e,g., OST, may then decompose and/or react in the proposed thin reaction zone at the gas-solid interface, producing the species composition measured near the surface with the MPMS system.

In Table 1, the post-flame region results for the present study and the work of Korobeinichev et al.[1] are compared to the results of equilibrium calculations performed with the equilibrium code.[23] The data of the present study given at 0.5 atmospheres was obtained by static sampling above the flame. The species composition in the post-flame region for the data of Korobeinichev et al.[1] deviated so much from the actual element fractions that rebalancing the data would have drastically changed the composition. As can be seen in Table 1, the post-flame composition at one atmosphere from the present study required substantial increases in the H_2 and H_2O mole fractions to balance the H fraction and a significant reduction in the amount of CO_2. These changes brought the balanced species composition relatively close to the equilibrium composition except for the large excess of NO observed and the lack of experimental observation of O_2 and the radicals H, O, and OH. Korobeinichev et al. also observed 0.03 mole fraction of NO in their products, possibly indicating that at these pressures combustion is not complete. The equilibrium calculations show that a considerable amount of H and OH radicals not detectable with the MPMS system are found in the equilibrium products. These radicals most likely are produced by the dissociation of H_2O at the temperatures of the final flame. The slight decrease in H_2O concentration above 800 μm displayed in Figure 2 supports to this hypothesis. The significant amount of H and OH in the gas products would also explain why for the MPMS test at one atmosphere the amount of H_2 and H_2O in the products had to be increased to balance the H fraction. The large excess of CO_2 versus the equilibrium composition appears to be only attributable to experimental error. However, it is interesting that Korobeinichev et al.[1] measured the exact same mole fraction of CO_2 in the post-flame region. The temperatures calculated for the MPMS results in the post-flame region were well above the equilibrium predictions. However, the last line in Table 1 shows that when the radicals and O_2 were excluded from the equilibrium code results when doing the enthalpy balance, the predicted gas temperature was well above the actual gas temperature. The gas temperature predicted by the MPMS results was relatively close to this temperature predicted by the equilibrium code when the radicals and O_2 were not considered.

KINETIC MODELLING OF RDX COMBUSTION

The PREMIX subroutine[8] in conjunction with the CHEMKIN software package[5-7] and the kinetic mechanism of Yetter and Dryer[11] was used to simulate the experimentally measured species profiles given in Figure 2. Several user inputs either from experimental observations or theoretical calculations were required to run the code. The mass flux from the surface was specified based on a burning rate of 0.11 cm/sec at the pressure and heat flux of the test depicted in Figure 2. An area expansion ratio for the gas plume was approximated based on previous studies[2,3] where a schlieren flow visualization system was used to visualize the gas-phase structure. The balanced gas composition and calculated gas-solid interface temperature given in Table 1 for the test at one atmosphere were used as initial conditions. The PREMIX code was run in the "burner-stabilized flame" format requiring the input of a temperature profile. No experimental measurements of temperature profiles for RDX were found in the literature. A profile for the self-deflagration of HMX presented by Hanson-Parr and Parr[25] showed a significant constant temperature region midway through the profile characteristic of a dark zone. This general shape of the profile was used initially as input to the present model of laser-induced RDX deflagration, but the resultant species profiles did not compare well to the data in Figure 2. This was to be expected since the measured species profiles of both the present study and the work of Korobeinichev et al.[1] showed no signs of a dark zone in the species profiles. Melius[9] calculated a roughly parabolic temperature profile in his modelling efforts where the energy equation was solved. As a first approximation, the parabolic temperature profile given in Figure 4 was used as

input to the present model. The profile was defined by starting at the calculated gas-solid interface temperature of 1075 K and reaching the equilibrium flame temperature of 2925 K at the vertex of the parabola at 2.0 millimeters.

Species profiles determined by the model are presented in Figure 4 and can be compared directly to the experimental results given in Figure 2. The comparison reveals that the Yetter and Dryer mechanism[11] produced excellent agreement between the model results and the experimental profiles. The profiles for H_2, H_2O, CH_2O, N_2O, and NO_2 are remarkably similar. The NO profile is also quite similar with a small increase in concentration in the primary flame and a steady decrease in the secondary flame starting at about 600 μm. The combination of N_2 and CO in a single experimental profile precluded any direct comparison of the model profiles for these two species. However, the production of CO by the model started at about 300 μm above the surface whereas the experimental profile for species at 28 amu did not begin to rise until 450-500 μm above the surface. The model results do not indicate any production of HCN in the primary flame zone as was experimentally observed.

The final composition determined by the model closely matched the equilibrium results given in Table 1 except for 0.045 mole fraction of NO which compares quite well with the experimental results. Final mole fractions of the minor species H, OH, O, and O_2 calculated by the model using the Yetter and Dryer mechanism were 0.029, 0.016, 0.003, and 0.002, respectively. All of these mole fractions were a bit lower than the equilibrium code results given in Table 1 but in general were quite good for calculations of minor species mole fractions. However, it is important to note that the final height for the model results is 3.0 millimeters but only 2.0 millimeters for the experimental results. For the modelling results, the chemistry in the primary flame appeared to be a bit faster as can be seen in the NO_2 profile. However, the model results were noticeably slower in the secondary flame than the experimental results. This most likely indicates that the assumed temperature profile was not totally accurate and that the temperature may reach the final flame value faster than the assumed parabolic profile. However, another possibility was that laser beam absorption by the reacting gases may drive the gas phase chemistry to occur more rapidly than is observed without any external heating as in the kinetic model. Price et al.[26] presented data for the absorption of CO_2 laser energy by various gases which indicated that HCN may exhibit significant absorption of the CO_2 laser beam. Since HCN is one of the primary participants in the luminous flame chemistry, its absorption of some beam energy may result in faster chemistry in this region for the laser-assisted combustion tests.

SUMMARY AND CONCLUSIONS

Both laser-induced regression (LIR) and laser-assisted combustion (LAC) conditions for RDX were investigated. Under LIR conditions, RDX displayed a large melt layer on the surface with considerable bubbling within the layer. The following species in descending order of abundance were detected within a gas bubble on the surface: CH_2O, N_2 and CO in a single peak at 28 amu, H_2O, NO_2, and N_2O with only small amounts of HCN and NO. Species were also detected at molecular weights of 42, 43, 54, 56, 70, 81, and 97 amu. LAC conditions were observed at 0.5 and 1.0 atmospheres if the heat flux was above 100 and 43 W/cm^2, respectively. The luminous flame appeared as a thin violet flame zone about 0.6 millimeters above the surface at one atmosphere with a heat flux of 100 W/cm^2 and about 5.0 millimeters above the surface at the same pressure and a heat flux of 1000 W/cm^2. Species profiles were measured which gave distinct evidence of a primary flame caused by reaction of CH_2O and NO_2 producing H_2, H_2O, HCN, NO, and CO_2. A gas-solid interface temperature of 1075 K was calculated. It was postulated that a thin unresolved reaction zone may exist directly above the surface where decomposition and reaction of RDX and/or large decomposition fragments of RDX may occur. The reaction in the luminous flame zone appeared to be due to HCN, NO, and to a lesser degree N_2O with H_2, H_2O, CO, N_2, and CO_2 produced. Modelling of the flame as a 1-D, premixed flame using a mechanism of 31 species and 152 reactions produced excellent agreement with the experimental profiles except that the luminous flame chemistry appeared to be slower than those observed experimentally. It was postulated that this may be due to laser heating of gas species which absorb well at the wavelength of the CO_2 laser such as HCN, thus enhancing the flame reactions.

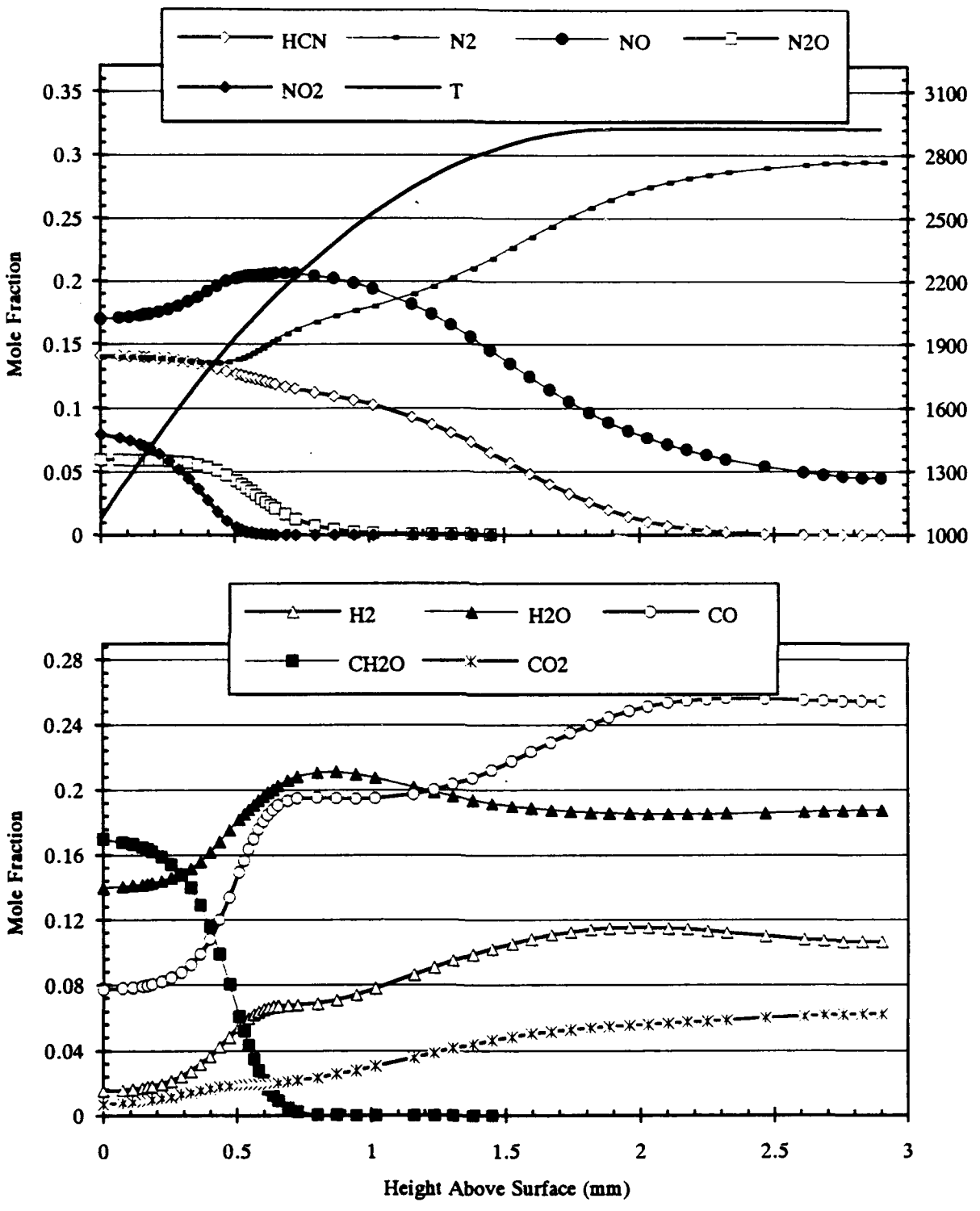

Figure 4. Species profiles generated by 1-D, premixed flame model of RDX deflagration. Initial conditions taken from experiments (P = 1 atm, q" = 100 W/sq cm). Parabolic temperature profile derived from enthalpy balance at surface and equilibrium calculation at infinity.

REFERENCES

1. Korobeinichev, O. P., Kuibida, L. V., Orlov, V. N., Tereschenko, A. G., Kutsenogii, K. P., Mavliev, R. A., Ermolin, N. E., Fomin, V. M., and Emel'yanov, I. D., "Mass Spectrometric Probe Study of the Flame Structure and Kinetics of Chemical Reactions in Flames," *Mass-Spektrom. Khim. Kinet.*, 1985, pp. 73-93.
2. Fetherolf, B. L. and Litzinger, T. A., "Physical and Chemical Processes Governing the CO_2 Laser-Induced Deflagration of Ammonium Dinitramide (ADN)," 29th JANNAF Combustion Meeting, CPIA Publ. 593, Vol. II, Oct. 1992, pp. 329-338.
3. Fetherolf, B. L., Liiva, P. M., Litzinger, T. A., and Kuo, K. K., "Thermal and Chemical Structure of the Preparation and Reaction Zones for RDX and RDX Composite Propellants," 28th JANNAF Combustion Meeting, CPIA Publ. 573, Vol. II, Oct. 1991, pp. 379-386.
4. Fetherolf, B. L., Litzinger, T. A., Lu, Y.-C., and Kuo., K. K., "A Comparison of the Physical and Chemical Processes Governing the CO_2 Laser-induced Pyrolysis and Deflagration of XM39 and M43," 30th JANNAF Combustion Meeting, November 1993.
5. Kee, R. J., Rupley, F. M., and Miller, J. A., "Chemkin-II: A Fortran Chemical Kinetics Package for the Analysis of Gas-Phase Chemical Kinetics," Sandia Report SAND89-8009, Sept. 1989.
6. Kee, R. J., Rupley, F. M., and Miller, J. A., "The Chemkin Thermodynamic Data Base," Sandia Report SAND87-8215B, March 1990, reprinted Dec. 1990.
7. Kee, R. J., Dixon-Lewis, G., Warnatz, J., Coltrin, M. E., and Miller, J. A., "A Fortran Computer code Package for the Evaluation of Gas-Phase Multi-component Transport Properties," Sandia Report SAND86-8246, Dec. 1986, reprinted Dec. 1990.
8. Kee, R. J., Gricar, J. F., Smooke, M. D., and Miller, J. A., "A Fortran Program for Modeling Steady Laminar One-Dimensional Premixed Flames," Sandia Report SAND85-8240, Dec. 1985, reprinted Oct. 1990.
9. Melius, C. F., "The Gas-Phase Flame Chemistry of Nitramine Combustion," 25th JANNAF Combustion Meeting, CPIA Publ. 498, Vol. II, Oct. 1988, pp. 155-162.
10. Ermolin, N. E., Korobeinichev, O. P., Kuibida, L. V., and Fomin, V. M., "Processes in Hexogene Flames," *Combustion, Explosion, and Shock Waves*, Vol. 24, No. 4, July-Aug. 1988, pp. 400-409.
11. Yetter, R. A., and Dryer, F. L., ONR Annual Report, 1993.
12. Fristrom, R. M., and Westenberg, A. A., Flame Structure, McGraw-Hill Book Co., 1965.
13. Boggs, T. L., "Thermal Behavior of RDX and HMX," Chapter 3 in Progress in Astronautics and Aeronautics: Fundamentals of Solid-Propellant Combustion, edited by K. K. Kuo and M. Summerfield, AIAA, Vol. 90, 1984, pp. 121-175.
14. Behrens, R., Jr., and Bulusu, S., "Thermal Decomposition of Energetic Materials. 4. Deuterium Isotope Effects and Isotopic Scrambling (H/D, $^{13}C/^{18}O$, $^{14}N/^{15}N$) in Condensed-Phase Decomposition of 1, 3, 5-Trinitrohexahydro-s-triazine," *Journal of Physical Chemistry*, Vol. 96, No. 22, 1992, pp. 8891-8897.
15. Schroeder, M. A., "Critical Analysis of Nitramine Decomposition Data: Product Distributions from HMX and RDX Decomposition," Technical Report BRL-TR-2659, June 1985, 117 pp.
16. Farber, M., and Srivastava, R. D., "Mass Spectrometric Investigation of the Thermal Decomposition of RDX," *Chemical Physics Letters*, Vol. 64, No. 2, July 1979, pp. 307-310.
17. Behrens, R., Jr., and Bulusu, S., "Thermal Decomposition of Energetic Materials. 3. Temporal Behaviors of the Rates of Formation of the Gaseous Pyrolysis Products from Condensed-Phase Decomposition of 1, 3, 5-Trinitro-hexahydro-s-triazine," *Journal of Physical Chemistry*, Vol. 96, No. 22, 1992, pp. 8877-8891.
18. Zhao, X., Hintsa, E. J., and Lee, Y. T., "Infrared Multiphoton Dissociation of RDX in a Molecular Beam," *Journal of Chemical Physics*, Vol. 88, No. 2, January 1988, pp. 801-810.
19. Goshgarian, B. B., "The Thermal Decomposition of Cyclotrimethylene-trinitramine (RDX) and Cyclotetramethylene-tetranitramine (HMX)," Technical Report AFRPL-TR-78-76, October 1978.
20. Oyumi, Y., and Brill, T. B., "Thermal Decomposition of Energetic Materials 3. A High-Rate, In Situ, FTIR Study of the Thermolysis of RDX and HMX with Pressure and Heating Rate as Variables," *Combustion and Flame*, Vol. 62, 1985, pp. 213-224.
21. Fifer, R. A., "Chemistry of Nitrate Ester and Nitramine Propellants," Chapter 4 in Progress in Astronautics and Aeronautics: Fundamentals of Solid-Propellant Combustion, edited by K. K. Kuo and M. Summerfield, AIAA, Vol. 90, 1984, pp. 177-237.

22. Snyder, A. P., Kremer, J. H., Liebman, S. A., Schroeder, M. A., and Fifer, R. A., "Characterization of Cyclotrimethylenetrinitramine (RDX) by N,H Isotope Analyses with Pyrolysis-Atmospheric Pressure Ionization Tandem Mass Spectrometry," *Organic Mass Spectrometry*, Vol. 24, 1989, pp. 15-21.
23. Gordon, S., and McBride, B. J., "Computer Program for Calculation of Complex Chemical Equilibrium Compositions, Rocket Performance, Incident and Reflected Shocks, and Chapman-Jouget Detonations," NASA SP-273, Interim Revision N78-17724, March 1976.
24. Brill, T. B., Brush, P. J., Patil, D. G., and Chen, J. K., "Chemical Pathways at a Burning Surface," Twenty-fourth Symposium (International) on Combustion, The Combustion Institute, 1992, pp. 1907-1914.
25. Hanson-Parr, D., and Parr, T., "Absorption Measurements in Propellant Flames," 28th JANNAF Combustion Meeting, CPIA Publ. 573, Vol. II, Oct. 1991, pp. 369-378.
26. Price, C. F., Atwood, A. I., and Parr, T. P., "The Role of External Radiation in the NWC Combustion Model," 28th JANNAF Combustion Meeting, CPIA Publ. 573, Vol. III, Oct. 1991, pp. 379-387.